

University of Groningen

## Structural analysis of flavinylation in vanillyl-alcohol oxidase

Fraaije, Marco; van den Heuvel, RHH; van Berkel, WJH; Mattevi, A; Heuvel, Robert H.H. van den; Berkel, Willem J.H. van

*Published in:*  
The Journal of Biological Chemistry

*DOI:*  
[10.1074/jbc.M004753200](https://doi.org/10.1074/jbc.M004753200)

**IMPORTANT NOTE: You are advised to consult the publisher's version (publisher's PDF) if you wish to cite from it. Please check the document version below.**

*Document Version*  
Publisher's PDF, also known as Version of record

*Publication date:*  
2000

[Link to publication in University of Groningen/UMCG research database](#)

*Citation for published version (APA):*

Fraaije, M. W., van den Heuvel, R. H. H., van Berkel, W. J. H., Mattevi, A., Heuvel, R. H. H. V. D., & Berkel, W. J. H. V. (2000). Structural analysis of flavinylation in vanillyl-alcohol oxidase. *The Journal of Biological Chemistry*, 275(49), 38654-38658. DOI: 10.1074/jbc.M004753200

**Copyright**

Other than for strictly personal use, it is not permitted to download or to forward/distribute the text or part of it without the consent of the author(s) and/or copyright holder(s), unless the work is under an open content license (like Creative Commons).

**Take-down policy**

If you believe that this document breaches copyright please contact us providing details, and we will remove access to the work immediately and investigate your claim.

*Downloaded from the University of Groningen/UMCG research database (Pure): <http://www.rug.nl/research/portal>. For technical reasons the number of authors shown on this cover page is limited to 10 maximum.*

## Structural Analysis of Flavinylation in Vanillyl-Alcohol Oxidase\*

Received for publication, June 1, 2000, and in revised form, August 18, 2000  
Published, JBC Papers in Press, September 12, 2000, DOI 10.1074/jbc.M004753200

Marco W. Fraaije<sup>‡§</sup>, Robert H. H. van den Heuvel<sup>¶</sup>, Willem J. H. van Berkel<sup>¶</sup>,  
and Andrea Mattevi<sup>‡</sup>

From the <sup>¶</sup>Department of Biomolecular Sciences, Laboratory of Biochemistry, Wageningen University, Dreijenlaan 3, 6703 HA Wageningen, The Netherlands and the <sup>‡</sup>Department of Genetics and Microbiology, University of Pavia, via Abbiategrasso 207, 27100 Pavia, Italy

Vanillyl-alcohol oxidase (VAO) is member of a newly recognized flavoprotein family of structurally related oxidoreductases. The enzyme contains a covalently linked FAD cofactor. To study the mechanism of flavinylation we have created a design point mutation (His-61 → Thr). In the mutant enzyme the covalent His-C8 $\alpha$ -flavin linkage is not formed, while the enzyme is still able to bind FAD and perform catalysis. The H61T mutant displays a similar affinity for FAD and ADP ( $K_d = 1.8$  and  $2.1 \mu\text{M}$ , respectively) but does not interact with FMN. H61T is about 10-fold less active with 4-(methoxymethyl)phenol ( $k_{\text{cat}} = 0.24 \text{ s}^{-1}$ ,  $K_m = 40 \mu\text{M}$ ) than the wild-type enzyme. The crystal structures of both the holo and apo form of H61T are highly similar to the structure of wild-type VAO, indicating that binding of FAD to the apoprotein does not require major structural rearrangements. These results show that covalent flavinylation is an autocatalytical process in which His-61 plays a crucial role by activating His-422. Furthermore, our studies clearly demonstrate that in VAO, the FAD binds via a typical lock-and-key approach to a preorganized binding site.

A substantial part of all biological reactions rely on the action of cofactor-dependent enzymes. By adding the functionality of a cofactor to the protein matrix, enzymes have found a way of expanding their catalytic power that has led to an enormous collection of different biocatalysts. For the various types of cofactors observed in nature, different molecular approaches of cofactor binding and anchoring have been identified. Flavoproteins represent one of the major groups of cofactor-dependent enzymes (1, 2). However, data on the molecular process of FAD or FMN binding are scarce, while only a limited number of flavoprotein structures in the apo form are known (3–5). A striking example of the importance of efficient FAD binding was recently shown for methylenetetrahydrofolate re-

ductase (6). A commonly found point mutation in the corresponding human gene results in a decreased cofactor affinity, which can lead to severe inborn health problems *e.g.* neural-tube defects and Down syndrome. For a better understanding of the process of flavin binding, we have started a study on the process of flavinylation in vanillyl-alcohol oxidase (VAO).<sup>1</sup>

VAO (EC 1.1.3.38) is a FAD-dependent enzyme capable of oxidizing a wide range of phenolic substrates providing the fungus *Penicillium simplicissimum* with a tool for metabolizing aromatic compounds (7). The structure of VAO encompasses 560 residues and a fully buried covalently bound FAD cofactor (Fig. 1) (8). The VAO monomer consists of two  $\alpha/\beta$  domains: residues 1–270 and 500–560 form a FAD binding domain, while the intervening residues form the so-called cap domain. The active site is located in the core of the protein, at the interface of the two domains with the flavin being covalently linked to His-422 of the cap domain. From a sequence alignment study it was recognized that VAO is a representative of a novel flavoprotein family, whose members share a conserved FAD binding domain (9). The recent unforeseen discovery of the same FAD binding fold in CO dehydrogenase indicates that this FAD binding module is widespread among flavoproteins (10).

Recently, we have performed an in-depth study on the role of the covalent histidyl-FAD bond in VAO (11). Covalent anchoring of a flavin cofactor has been encountered in a variety of other flavin-dependent oxidoreductases, while the rationale for this type of cofactor attachment has remained obscure for a long time (12). Our recent study showed that deletion of the histidyl bond, by replacing His-422 by an alanine, resulted in an active VAO variant containing a noncovalently but tightly bound FAD cofactor. Determination of the structure of this mutant enzyme revealed that rupture of the covalent link does not have any effect on the active site architecture or any other part of the protein structure. Kinetic analysis, however, revealed that the mutant enzyme displays a 10-fold decrease in activity, which is due to a significantly lowered flavin redox potential ( $-65 \text{ mV}$ ) with respect to the wild-type enzyme ( $+55 \text{ mV}$ ). This drastic decrease in redox potential can fully explain the altered flavin reactivity, indicating that the covalent tethering of the cofactor might have evolved to fine tune the redox properties of the cofactor.

In the process of covalent His<sup>422</sup>-FAD bond formation, His-61 is thought to play an important role (8, 13). His-61 is envisaged to deprotonate the neighboring His-422 as the shortest distance between the imidazole rings is only about  $2.5 \text{ \AA}$ . By this, His-422 is able to attack the activated  $8\alpha$ -methyl group of the FAD cofactor creating the covalent linkage (12). To examine the functional role of His-61 in the process of flavinylation, we

\* This work was supported by grants from Ministero dell' Università e Ricerca Scientifica e Tecnologica (Project "Biologia Strutturale e Dinamica di Proteine Redox"), Consiglio Nazionale delle Ricerche (CNR target project on "Biotechnology"), Agenzia Spaziale Italiana, and a European Molecular Biology postdoctoral fellowship (to M. W. F.). The costs of publication of this article were defrayed in part by the payment of page charges. This article must therefore be hereby marked "advertisement" in accordance with 18 U.S.C. Section 1734 solely to indicate this fact.

The atomic coordinates and structure factors (codes 1E8F, 1E8G, and 1E8H) have been deposited in the Protein Data Bank, Research Collaboratory for Structural Bioinformatics, Rutgers University, New Brunswick, NJ (<http://www.rcsb.org/>).

§ To whom correspondence should be addressed: Laboratory of Biochemistry, University of Groningen, Nijenborgh 4, 9747 AG Groningen, The Netherlands. Tel.: 31-503634345; Fax: 31-503634165; E-mail: m.w.fraaije@chem.rug.nl.

<sup>1</sup> The abbreviation used is: VAO; vanillyl-alcohol oxidase.

have substituted this residue by a threonine. In this paper, we report on the structural and catalytic properties of the H61T mutant. Furthermore, it presents the first x-ray structural studies of an apo form of a flavoenzyme that normally contains a covalent FAD cofactor.

#### EXPERIMENTAL PROCEDURES

**Chemicals, Bacterial Strains, and Plasmids**—*Escherichia coli* strain DH5F' and the plasmids pUCBM20 (Roche Molecular Biochemicals) and pGEM-5Zf(+) (Promega) were used for cloning throughout, whereas *E. coli* strain TG2 and the plasmid pEMBL19(-) (Roche Molecular Biochemicals) were used for expression of the *vaoa* gene. Oligonucleotides, T4 DNA ligase, restriction enzymes, isopropyl- $\beta$ -D-thiogalactopyranoside, yeast extract, and tryptone extract were from Life Technologies, Inc. Forward M13 and reverse M13 sequencing primers

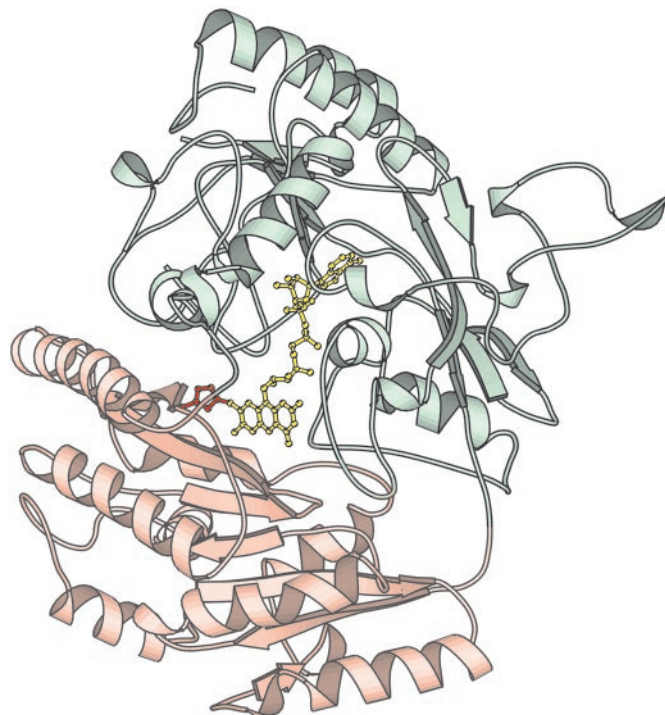


FIG. 1. Ribbons diagram of the overall structure of the VAO monomer. The FAD-binding domain is shown in green, and the cap domain is shown in red. The histidyl-bound FAD cofactor is shown in ball-and-stick model. The picture was produced with MOLSCRIPT (26).

were from Amersham Pharmacia Biotech. *Pwo* DNA polymerase and dNTPs were purchased from Roche Molecular Biochemicals, and Super *Taq* DNA polymerase was purchased from HT Biotechnology. Ampicillin, riboflavin, ADP, AMP, FMN, NAD<sup>+</sup>, and NADP<sup>+</sup> were from Sigma. 4-(Methoxymethyl)phenol was obtained from Aldrich. All other chemicals were from Merck and were of the purest grade available.

**Analytical Methods**—Site-directed mutagenesis was performed as described previously (11). For the His-61 replacement by polymerase chain reaction-based mutagenesis, the oligonucleotide 5' CGCACGATCCCACTCATGTCATGGACCAGG 3' (where ACT denotes the His-61  $\rightarrow$  Thr replacement) was used. Successful mutagenesis was confirmed by plasmid sequencing. The H61T mutant protein was expressed and purified as described previously (11). By extensive gel permeation of holo H61T, virtually all FAD could be released. The FAD content in the apoprotein preparations was <0.1% as evidenced by the flavin absorbance at 439 nm. Steady-state kinetic parameters of H61T were determined by using saturating conditions for cofactor binding (100  $\mu$ M FAD), essentially as described earlier (7). Tryptophan fluorescence was measured using a Aminco SPF-500 fluorimeter.

**Crystallization**—Crystals were obtained using the hanging-drop vapor diffusion method at similar conditions (4% w/v polyethylene glycol 4000, 100 mM sodium acetate/HCl, pH 5.1) that were used for crystallizing wild-type VAO (14). Crystals of the H61T mutant in both the apo and the holo form (size typically  $\sim 0.2 \times 0.2 \times 0.3$  mm<sup>3</sup>) were isomorphous to those of wild-type enzyme, and they belong to space group I4.

**Data Collection, Structural Determination, and Refinement**—A complete data set was collected at 100 K using a single crystal. Before freezing, the crystals were briefly transferred to a solution containing 10% w/v polyethylene glycol 400, 5% w/v polyethylene glycol 4000, 10% v/v glycerol, and 100 mM acetate/HCl, pH 5.1. Data were measured on the following beam lines: beam line X11 of the Deutsches Elektronen-Synchrotron/European Molecular Biology Laboratory (Hamburg, Germany) for the holoprotein crystal soaked in 1.0 mM 4-(trifluoromethyl)phenol and beam line ID14-EH3 of European Synchrotron Radiation Facility (Grenoble, France) for the apoprotein and the apoprotein soaked in 1.0 mM ADP. The structures were solved by difference Fourier methods and maximum likelihood refinement using REFMAC (15) and other CCP4 programs (16). Model building was carried out using the program O (17), whereas positions of ordered water were identified using the ARP program (18). Table I gives a summary of the final refinement statistics. The free *R*-factor was calculated employing the same reflections used for the free *R*-factor calculations in the refinement of the wild-type structure.

**Coordinates**—Coordinates have been deposited in the Protein Data Bank (accession codes 1E8F, 1E8G, and 1E8H).

#### RESULTS AND DISCUSSION

**Characterization of the His-61  $\rightarrow$  Thr VAO Mutant**—Purification and characterization of H61T revealed that the mutation did not abolish enzyme activity. However, it was found that

TABLE I  
Statistics from the crystallographic analysis

Data set	Apoenzyme	ADP complex	Holoenzyme
Resolution range (Å)	20–2.9	20–2.6	15–2.1
Observed reflections	54479	85638	151791
Unique reflections	23727	34320	57201
Data completeness (%) <sup>a</sup>	98.1 (98.1)	99.8 (99.6)	98.9 (99.7)
Multiplicity	2.3 (2.2)	2.5 (2.5)	2.5 (2.5)
Intensities ( <i>I</i> / $\sigma$ )	5.2 (1.9)	5.2 (2.2)	5.9 (2.4)
<i>R</i> <sub>sym</sub> (%) <sup>a,b</sup>	10.5 (38.5)	9.0 (33.0)	6.6 (23.3)
Cell dimensions (Å)	<i>a</i> = <i>b</i> = 129.28 <i>c</i> = 130.40	<i>a</i> = <i>b</i> = 130.34 <i>c</i> = 134.00	<i>a</i> = <i>b</i> = 130.29 <i>c</i> = 132.54
<i>R</i> -factor (%)	23.9	23.7	21.8
<i>R</i> <sub>free</sub> (%)	31.6	30.3	25.8
Number of water atoms	20	90	396
Number of ligand atoms	0	54 (ADP)	106 (FAD)
r.m.s.d. from ideality <sup>c</sup>			22 (4-(Trifluoromethyl)phenol)
Bond lengths (Å)	0.012	0.011	0.010
Bond angles (°)	2.8	2.4	2.2
Trigonal groups (Å)	0.023	0.021	0.020
Planar groups (Å)	0.011	0.010	0.009
Ramachandran plot (%) <sup>d</sup>	83.3/16.7/0	86.2/13.8/0	89.7/10.3/0

<sup>a</sup> The values relating to the highest resolution shell are given in parentheses.

<sup>b</sup>  $R_{\text{sym}} = I_j \langle I_j \rangle / \langle I_j \rangle$ , where  $I_j$  is the intensity of an observation of reflection  $j$  and  $\langle I_j \rangle$  is the average intensity for reflection  $j$ .

<sup>c</sup> The root mean square deviations (r.m.s.d.) were calculated using the program REFMAC (15).

<sup>d</sup> Percentage of residues in most favored, allowed, and disallowed regions of the Ramachandran plot as checked with the program PROCHECK (19).

TABLE II  
Steady-state kinetic parameters of wild-type, H422A and H61T VAO for the oxidation of 4-(methoxymethyl)phenol (50 mM potassium phosphate buffer, pH 7.5, 25 °C)

Parameter	Wild-type <sup>a</sup>	H422A <sup>b</sup>	H61T
$K_m$ ( $\mu\text{M}$ )	55	34	40
$k_{\text{cat}}$ ( $\text{s}^{-1}$ )	3.1	0.27	0.24
$k_{\text{cat}}/K_m$ ( $\text{mM}^{-1}\cdot\text{s}^{-1}$ )	56	7.9	6.0

<sup>a</sup> Data from Ref. 7.

<sup>b</sup> Data from Ref. 11.

during the purification the protein readily lost activity, which could be restored by supplementing the protein solution with FAD. This indicated that the mutant has only a moderate affinity for FAD. Unfolding of the purified protein confirmed that no covalently bound FAD is formed in the H61T mutant confirming the crucial role of this residue in the autocatalytical covalent tethering of the prosthetic group. Kinetic analysis revealed that the turnover rate of H61T was decreased by 1 order of magnitude when compared with wild-type VAO (Table II). The effect on enzyme activity can well be explained by an decreased redox potential of the cofactor due to the missing covalent bond (11). In fact, the observed effect on the activity was anticipated as it has been shown that merely disruption of the covalent His-FAD bond results in a 10-fold decrease in activity due to a changed redox potential of the cofactor, while the mutation was not expected to have a direct effect on the catalytic function of the enzyme as the respective residue is far from the active site (distance between the imidazole ring of His-61 and the FAD N5 atom is  $>10$  Å). Unfortunately, attempts to determine the redox potential of the mutant enzyme were unsuccessful due to the moderate affinity for FAD. As a consequence a solution of the mutant enzyme contains relatively large amounts of unbound FAD. Spectral interference of the fraction of free FAD prevented an unambiguous redox potential determination of the mutant enzyme.

The binding affinity for FAD to the mutant enzyme was determined using tryptophan fluorescence quenching:  $K_d = 1.8$   $\mu\text{M}$ . The noncovalent binding of the FAD cofactor could also be demonstrated by the inhibitory effects of some FAD-related compounds. Of all tested FAD derivatives (riboflavin, FMN,  $\text{NAD}^+$ ,  $\text{NADP}^+$ , AMP, and ADP) only the addition of AMP or ADP resulted in a decreased enzyme activity. ADP was found to be an effective competitive inhibitor, indicating that the FAD binding largely depends on binding of the ADP moiety of the cofactor, a frequently observed feature in FAD binding enzymes (20–22). Binding of ADP could also be measured by using tryptophan fluorescence, showing a similar affinity ( $K_d = 2.1$   $\mu\text{M}$ ) when compared with FAD. The data for both FAD and ADP binding were consistent with a single site binding process. However, binding of ADP resulted in less fluorescence quenching. This might be related to the fact that in the VAO structure, Trp-413 is close to the isoalloxazine ring of FAD.

Due to the impairment in covalent flavinylation, the apo form of H61T could be purified in large amounts, which opened up possibilities to explore the process of FAD binding. Both the apo and the holo form of H61T showed similar hydrodynamic behavior: they form octamers of about 500 kDa (23) and can be crystallized using similar conditions as found for wild-type enzyme. By solving the crystal structures of both the apo- and the holoenzyme (Table I), we have been able to examine the structural effects associated with FAD binding.

**Structure of the His-61  $\rightarrow$  Thr VAO Holoenzyme**—Comparison of the mutant holo form structure with the previously solved wild-type structure (8) established that the His-61 replacement and the resulting missing covalent histidyl-FAD bond does not induce gross conformational changes. Except for

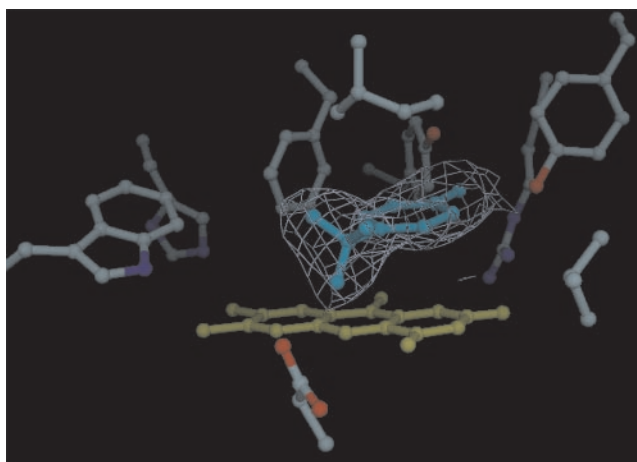


FIG. 2. The active site of the H61T ternary complex structure showing all relevant residues, the isoalloxazine ring of the FAD cofactor (yellow) and the bound 4-(trifluoromethyl)phenol (blue) contoured by the  $2F_o - F_c$  electron density calculated with the refined model. The picture was generated with DINO (27).

a perturbation in the loop region Met<sup>64</sup>–Tyr<sup>68</sup>, displaying a maximal shift of 4.5 Å, the  $\text{C}\alpha$  atoms superimpose with a root mean square deviation of 0.46 Å for 910 equivalent positions (*i.e.* the two VAO subunits present in the asymmetric unit). The loop movement is far from both the cofactor, and the active site and is probably caused by altered interactions due to the mutation. The active site architecture and mode of flavin binding of H61T is strictly conserved when compared with the wild-type enzyme. These observations support the notion that by mutating His-61 we have specifically inhibited the process of covalent flavinylation, while the mutant has retained appreciable activity. This also illustrates the dual catalytic potential of VAO as the enzyme is able to catalyze two totally different redox reactions: formation of the covalent histidyl-FAD bond and oxidation of phenolic compounds. To explore the conservation of substrate binding, the crystals of holo H61T were soaked in a solution containing 4-(trifluoromethyl)phenol, a competitive inhibitor. Inspection of the electron density map showed strong density for a bound 4-(trifluoromethyl)phenol molecule in the active site. The benzylic ring of the substrate analog is stacked almost parallel to the plane of the isoalloxazine ring ( $13^\circ$ ), while the phenolic oxygen makes a hydrogen bond with Tyr-503. As all fluorine atoms are resolved, it can be nicely seen that one fluorine atom is directly pointing toward the reactive N5 atom of the flavin ring (Fig. 2). The distance between the  $\text{C}\alpha$  atom and the flavin N5 atom (3.7 Å) and the angles  $\text{C}\alpha$ -F-N5 ( $132^\circ$ ) and  $\text{C}\alpha$ -N5-N10 ( $114^\circ$ ) are fully compatible with a direct hydride transfer, which is in line with the previously proposed catalytic mechanism (7). Moreover, the observed orientation of the ligand is similar to the binding mode of phenolic inhibitors in other complexed VAO structures (8), confirming conservation of the active site architecture. To exemplify the high degree of similarity of inhibitor binding between different liganded VAO structures, the isoeugenol complexed structures of wild-type VAO (8) and the H422A VAO variant (11) (Protein Data Bank entries 2VAO and 1QLU, respectively) were compared with the 4-(trifluoromethyl)phenol complexed H61T structure. Analysis of the superimposed active sites yields the following key parameters for inhibitor binding: the hydrogen bond distances between Tyr-503 and the hydroxyl group of the ligands are 2.4, 2.7, and 2.5 Å respectively, the distances between flavin N5 and the  $\text{C}\alpha$  atom of the inhibitor is 3.5, 3.5, and 3.7 Å, respectively, while the phenolic ring is at a conserved angle with respect to the plane of the isoalloxazine ring (18, 8, and  $13^\circ$ , respectively).

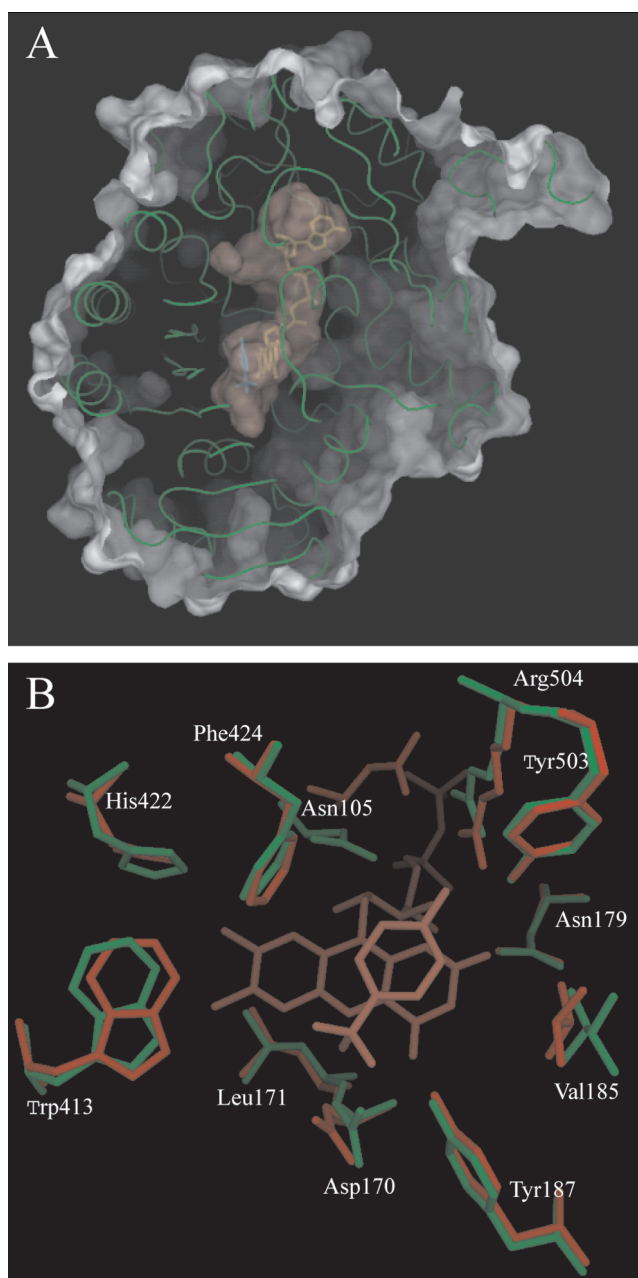


FIG. 3. *A*, a section through the  $C\alpha$  trace of the apoenzyme subunit showing the large internal solvent-filled cavity. For clarity, the FAD cofactor and 4-(trifluoromethyl)phenol as bound in the holo H61T ternary complex were superimposed and shown in *yellow* and *blue*, respectively. The surface was calculated using MSMS (28) and the picture was generated using DINO (27). *B*, superposition of active site residues in the apo (*green*) and the holo form complexed with 4-(trifluoromethyl)phenol (*red*) structures of the VAO H61T mutant. The figure was prepared with MOLSCRIPT (26).

**Structure of the Apoenzyme**—Structure determination of the apo form of H61T revealed a remarkable detailed resemblance with the holoenzyme structure. Superposition of the  $C\alpha$  atoms did not reveal any significant cofactor-induced conformational change, which is reflected in a root mean square deviation of only 0.33 Å. Consequently, a huge solvent-filled cavity (420 Å<sup>3</sup>) is found in the apoenzyme structure complementary with the missing cofactor (Fig. 3A). When the effect of FAD binding on the active site architecture is taken under scrutiny, only a few notable changes can be observed when compared with the holoenzyme (Fig. 3B). Particularly, comparison between the mutant holo and apo form structures shows that only the side

chains of Asn-105 and Ser-106 have altered positions, whereas all other active site residues superimpose with a root mean square deviation of <0.4 Å. These results indicate that, prior to binding of the cofactor, the apoprotein is fully folded, awaiting FAD binding.

Along with the apoenzyme structure, also the structure of the binary complex with ADP was determined at 2.6 Å. Similar to FAD binding, binding of ADP did not induce any structural changes as evidenced by a root mean square deviation of only 0.30 Å for all  $C\alpha$  atoms when compared with the apoenzyme structure.

**Holoenzyme Assembly**—The cofactor binding capability of the folded apoprotein could be demonstrated by soaking the colorless apoenzyme crystals in a FAD containing solution. Binding of FAD was completed within a few minutes as subsequent washing of the FAD soaked crystals resulted in bright yellow crystals. Furthermore, these FAD reconstituted enzyme crystals were also active as evidenced by substrate oxidation upon incubation with 4-(methoxymethyl)phenol. Apparently, the folded apoenzyme, even in the crystalline state, is malleable enough to allow the relatively large cofactor to enter the preorganized binding pocket resulting in the active holoenzyme. However, although the active site is nearly conserved in the apo form, soaking of apoenzyme crystals with substrate analogs did not result in ligand binding. This indicates that the positioning of the isoalloxazine ring system is a prerequisite for substrate binding, which is different from the situation in *e.g.* *p*-hydroxybenzoate hydroxylase (24, 25).

The similarity between the mutant structures in the holo and apo form clearly indicate that FAD binding does not involve an induced fit mechanism nor that the cofactor is required to attain the catalytically relevant conformation of the active site. Rather, both cofactor and substrate bind via a typical lock-and-key approach to highly preorganized binding sites. The observed lock-and-key mechanism for FAD binding is likely to apply to other flavoproteins. In particular, analysis of the recently discovered flavoprotein family of VAO related protein sequences shows that the most conserved residues are lining the FAD binding pocket (9), suggesting conservation in the mechanism of flavinylolation.

The reported crystallographic data provide detailed insight in the protein-ligand interactions involved in flavin-mediated catalysis. Combined with the recently solved structures of VAO, we now have a clear view on the molecular trajectory of enzyme assembly in VAO, which is composed of the following steps: 1) the polypeptide folds and oligomerizes (23) to yield apoprotein, 2) FAD is encapsulated by a highly preorganized cofactor binding cavity, 3) autocatalytical covalent flavinylolation results in cofactor activation enabling efficient redox catalysis. By this, we have gained valuable information on the process of flavin binding that will aid in understanding the biological process of cofactor recognition, binding, and subsequent activation of apoenzymes.

**Acknowledgments**—We gratefully acknowledge the beam time provided by the European Synchrotron Radiation Facility and Deutsches Elektronen-Synchrotron synchrotrons.

#### REFERENCES

- Ghisla, S., and Massey, V. (1989) *Eur. J. Biochem.* **181**, 1–17
- Fraaije, M. W., and Mattevi, A. (2000) *Trends Biochem. Sci.* **25**, 126–132
- Sandalova, T., and Lindqvist, Y. (1993) *FEBS Lett.* **327**, 361–365
- Steensma, E., and van Mierlo, C. P. M. (1998) *J. Mol. Biol.* **282**, 653–666
- Mattevi, A., Tedeschi, G., Bacchella, L., Coda, A., Negri, A., and Ronchi, S. (1999) *Struct. Fold. Des.* **7**, 745–756
- Guenther, B. D., Sheppard, C. A., Tran, P., Rozen, R., Matthews, R. G., and Ludwig, M. L. (1999) *Nat. Struct. Biol.* **6**, 359–365
- Fraaije, M. W., and van Berkel, W. J. H. (1997) *J. Biol. Chem.* **272**, 18111–18116
- Mattevi, A., Fraaije, M. W., Mozzarelli, A., Olivi, L., Coda, A., and van Berkel, W. J. H. (1997) *Structure* **5**, 907–920

9. Fraaije, M. W., van Berkel, W. J. H., Benen, J. A., Visser, J., and Mattevi, A. (1998) *Trends Biochem. Sci.* **23**, 206–207
10. Dobbek, H., Gremer, L., Meyer, O., and Huber, R. (1999) *Proc. Natl. Acad. Sci. U. S. A.* **96**, 8884–8889
11. Fraaije, M. W., van den Heuvel, R. H. H., van Berkel, W. J. H., and Mattevi, A. (1999) *J. Biol. Chem.* **274**, 35514–35520
12. Mewies, M., McIntire, W. S., and Scrutton, N. S. (1998) *Protein Sci.* **7**, 7–20
13. Trickey, P., Wagner, M. A., Jorns, M. S., and Mathews, F. S. (1999) *Struct. Fold. Des.* **7**, 331–345
14. Mattevi, A., Fraaije, M. W., Coda, A., and van Berkel, W. J. H. (1997) *Proteins Struct. Funct. Genet.* **27**, 601–603
15. Murshudov, G. N., Vagin, A. A., and Dodson, E. J. (1997) *Acta Crystallogr. Sect. D Biol. Crystallogr.* **53**, 240–255
16. Collaborative Computational Project Number 4 (1994) *Acta Crystallogr. Sect. D Biol. Crystallogr.* **50**, 760–767
17. Jones, T. A., Zou, J.-Y., Cowan, S. W., and Kjeldgaard, M. (1991) *Acta Crystallogr. Sect. A* **47**, 110–119
18. Lamzin, V. S., and Wilson, K. S. (1993) *Acta Crystallogr. Sect. D Biol. Crystallogr.* **49**, 129–147
19. Morris, A. L., MacArthur, M. W., Hutchinson, E. G., and Thornton, J. M. (1992) *Proteins Struct. Funct. Genet.* **12**, 345–364
20. van der Laan, J. M., Schreuder, H. A., Swarte, M. B., Wierenga, R. K., Kalk, K. H., Hol, W. G., and Drenth, J. (1989) *Biochemistry* **28**, 7199–7205
21. Sato, K., Nishina, Y., and Shiga, K. (1992) *J. Biochem. (Tokyo)* **112**, 804–810
22. Tedeschi, G., Negri, A., Ceciliani, F., Mattevi, A., and Ronchi, S. (1999) *Eur. J. Biochem.* **260**, 896–903
23. van Berkel, W. J. H., van den Heuvel, R. H. H., Versluis, C., and Heck, A. J. R. (2000) *Protein Sci.* **9**, 435–441
24. Müller, F., and van Berkel, W. J. H. (1982) *Eur. J. Biochem.* **128**, 21–27
25. Schreuder, H. A., Mattevi, A., Obmolova, G., Kalk, K. H., Hol, W. G., van der Bolt, F. J. T., and van Berkel, W. J. H. (1994) *Biochemistry* **33**, 10161–10170
26. Kraulis, P. (1991) *J. Appl. Crystallogr.* **24**, 946–950
27. DINO: Visualizing Structural Biology (1999) <http://www.bioz.unibas.ch/~xray/dino>
28. Sanner, M. F., Olson, A. J., and Spenger, J.-C. (1995) *Biopolymers* **38**, 305–320